10-1-2022

Incisionless targeted adeno-associated viral vector delivery to the brain by focused ultrasound-mediated intranasal administration

Dezhuang Ye

Jinyun Yuan

Yaoheng Yang

Yimei Yue

Zhongtao Hu

See next page for additional authors

Authors

Dezhuang Ye, Jinyun Yuan, Yaoheng Yang, Yimei Yue, Zhongtao Hu, Siaka Fadera, and Hong Chen

Incisionless targeted adeno-associated viral vector delivery to the brain by focused ultrasound-mediated intranasal administration

Dezhuang Ye,[a] Jinyun Yuan,[a] Yaoheng Yang,[a] Yimei Yue,[a] Zhongtao Hu,[a] Siaka Fadera,[a] and Hong Chen [a,b]*

[a]Department of Biomedical Engineering, Washington University in St. Louis, Saint Louis, MO 63130, USA
[b]Department of Radiation Oncology, Washington University School of Medicine, Saint Louis, MO 63108, USA

eBioMedicine 2022;84: 104277
Published online 21 September 2022
https://doi.org/10.1016/j.ebiom.2022.104277

Summary

Background Adeno-associated viral (AAV) vectors are currently the leading platform for gene therapy with the potential to treat a variety of central nervous system (CNS) diseases. There are numerous methods for delivering AAVs to the CNS, such as direct intracranial injection (DI), intranasal delivery (IN), and intravenous injection with focused ultrasound-induced blood–brain barrier disruption (FUS-BBBD). However, non-invasive and efficient delivery of AAVs to the brain with minimal systemic toxicity remain the major challenge. This study aims to investigate the potential of focused ultrasound-mediated intranasal delivery (FUSIN) in AAV delivery to brain.

Methods Mice were intranasally administered with AAV5 encoding enhanced green fluorescence protein (AAV5-EGFP) followed by FUS sonication in the presence of systemically injected microbubbles. Mouse brains and other major organs were harvested for immunohistological staining, PCR quantification, and in situ hybridization. The AAV delivery outcomes were compared with those of DI, FUS-BBBD, and IN delivery.

Findings FUSIN achieved safe and efficient delivery of AAV5-EGFP to spatially targeted brain locations, including a superficial brain site (cortex) and a deep brain region (brainstem). FUSIN achieved comparable delivery outcomes as the established DI, and displayed 414.9-fold and 2073.7-fold higher delivery efficiency than FUS-BBBD and IN. FUSIN was associated with minimal biodistribution in peripheral organs, which was comparable to that of DI.

Interpretation Our results suggest that FUSIN is a promising technique for non-invasive, efficient, safe, and spatially targeted AAV delivery to the brain.

Funding National Institutes of Health (NIH) grants R01EB027223, R01EB030102, R01MH116981, and UG3MH126861.

Keywords: Adeno-associated viral vectors; Blood–brain barrier; Gene therapy; Focused ultrasound; Intranasal delivery

Introduction

Gene therapy using adeno-associated viral vectors (AAVs) is one of the most promising therapeutic innovations for treating central nervous system (CNS) diseases.[1,2] However, there is a lack of non-invasive methods for efficient delivery of AAVs to the brain, which limits the development of CNS gene therapy. One of the major challenges in delivering AAVs to the brain is surmounting the blood–brain barrier (BBB). The BBB functions as a gatekeeper that only permits the transport of essential molecules from the blood to the brain. Most therapeutic agents, including AAVs, cannot permeate through the BBB.

Several strategies have been tested to overcome the BBB for AAV delivery to the brain. Direct intracranial injection (DI) of AAVs provides high delivery efficiency to the injected brain site and low systemic distribution to peripheral organs, but the resulting neuronal transduction is limited to a small region surrounding the injection site. DI requires invasive surgical procedures, which carry a risk for infection, bleeding, and edema, and pose technical challenges for viral delivery to critical brain locations (e.g., brainstem that controls essential

*Corresponding author at: Department of Biomedical Engineering and Radiation Oncology, Washington University in St. Louis. 4511 Forest Park Ave. St. Louis, MO 63108, USA.
E-mail address: hongchen@wustl.edu (H. Chen).

Research in context

Evidence before this study

Adeno-associated virus (AAV) vectors are the most frequently used viral vectors for gene therapy. With the recent United State Food and Drug Administration (USFDA) approval of several AAV-based gene therapies, there is an expanding number of AAV-based gene therapy clinical trials. However, the lack of non-invasive techniques for efficient delivery of AAVs to the brain with minimal toxicity to the peripheral organs poses the major bottleneck in the development of CNS-targeted gene therapy. The commonly used direct intracranial injection of AAV is invasive, and the expression is limited to the injection region. Intravenous injection of AAVs requires a unique blood–brain barrier-permeable capsid design and suffers from the risks of systemic toxicity associated with intravenous injection. Focused ultrasound-induced blood–brain barrier disruption can achieve non-invasive and spatially targeted AAV delivery to the brain, but it faces critical challenges of low delivery efficiency and high risk of peripheral exposure.

Added-value of this study

This study demonstrated that focused ultrasound-mediated intranasal delivery (FUSIN) achieved non-invasive and spatially targeted delivery of AAVs to targeted brain locations with high delivery efficiency and minimal biodistribution in peripheral organs.

Implications of all the available evidence

There is a direct pathway for translating FUSIN to the clinic because the foundational techniques, including FUS-mediated brain drug delivery, intranasal administration, and gene therapy with AAVs, have all been applied in humans. This gene delivery technique can potentially transform AAV delivery to the brain and accelerate the development of CNS-targeted gene therapy.

life functions such as breathing and heart rate).[3] Another strategy is directly injecting AAVs into the cerebrospinal fluid (CSF) compartment. This method provides more widespread gene expression than DI, but still requires surgical intervention, and the delivered AAVs may transduce the spinal cord region.[4] Non-invasive delivery via intravenous injection (IV) became an attractive approach with the development of BBB-permeable AAV vectors. Unfortunately, the trans-BBB function of these AAV vectors depends on the animal species and strains, which limits their broad application.[5,6] The IV route also requires large injection doses due to renal and hepatic clearance, which raises concerns of systematic toxicity.[7,8] Focused ultrasound (FUS) combined with microbubble-induced BBB disruption (FUS-BBBD) has been used for non-invasive and localized delivery of IV-injected agents, and ongoing clinical trials are testing the delivery of several therapeutic drugs.[9-12] Recent small animal studies showed that FUS-BBBD achieved higher AAV delivery efficiency to a targeted brain location than IV injection alone[13-16]; however, the systemic biodistribution associated with IV injection still poses challenges in its application.

Intranasal (IN) delivery is a non-invasive drug and gene delivery approach. It directly delivers therapeutic agents from the nose to the brain by utilizing the olfactory and trigeminal nerve pathways, bypassing the BBB and minimizing systemic exposure.[17] However, IN delivery is limited by low delivery efficiency and not specifically targeting the diseased brain region.[18,19] FUS-mediated intranasal delivery (FUSIN) can overcome these limitations and achieve efficient therapeutic agent delivery to spatially targeted brain regions. FUS utilizes ultrasound waves that can penetrate the scalp and skull to target virtually any location inside the brain, where it induces IV injected microbubble expansion and contraction that push and pull on the adjacent blood vessel wall.[20] These mechanical interactions generate a microbubble pumping effect, which is hypothesized to enhance penetration and subsequent accumulation of IN-administered drugs by convective mixing (Figure 1). Although FUSIN utilizes the same mechanical

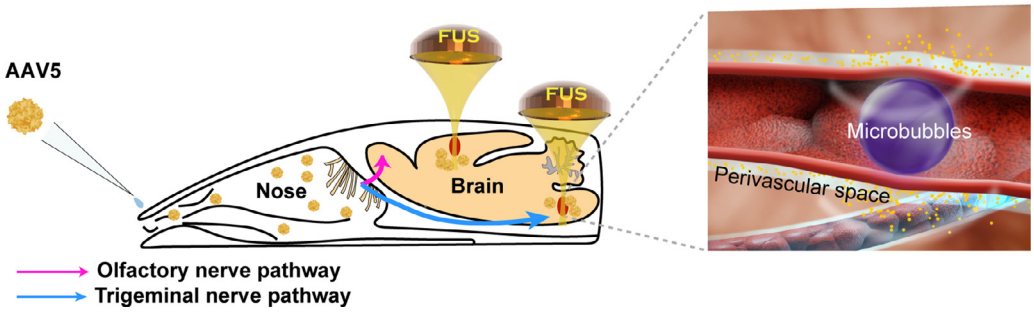

Figure 1. Illustration of focused ultrasound-mediated intranasal delivery (FUSIN) of AAV5-hSyn-EGFP to the mouse brain. FUSIN is a promising technique for non-invasive, efficient, and spatially targeted AAV delivery to the brain.

interactions among FUS, microbubbles, and blood vessels as conventional FUS-BBBD, it differs from FUS-BBBD in two critical aspects: (1) FUSIN utilizes the nose-to-brain pathway, which achieves direct therapeutic agent transport from the nose to the brain, whereas FUS-BBBD utilizes the blood-to-brain pathway; (2) FUSIN aims to enhance the penetration of therapeutic agents that are already at the perivascular space beyond the BBB,[21,22] whereas FUS-BBBD aims to mechanically disrupt the BBB. The FUSIN procedure is entirely non-invasive: the only operations on the animal are to remove the fur on the head for acoustic coupling, and to inject microbubbles into the tail vein. FUSIN has successfully delivered multiple agents, including dextrans, gold nanoparticles, and protein drugs, to different brain regions with high efficiency and minimal systemic exposure.[23–25] However, no study has been performed to evaluate its potential for AAV delivery.

The objective of this study was to evaluate the potential of FUSIN for non-invasive and efficient delivery of AAVs to the mouse brain. AAVs may utilize the nasal pathway to reach the brain directly, and FUS sonication has the potential to enhance their delivery efficiency at the targeted brain region. We first demonstrated successful FUSIN delivery of AAV5 encoding enhanced green fluorescence protein (EGFP) under the control of the human Synapsin 1 promoter (AAV5-hSyn-EGFP). We then compared FUSIN with DI (the most frequently used approach for brain AAV delivery), FUS-BBBD, and IN delivery and analyzed their delivery efficiency to the brain and biodistribution to other major organs. The potential of FUSIN as a platform technique for AAV delivery was demonstrated by the delivery of AAVs to both a superficial target (cortex) and a deep brain target (brainstem).

Methods

Ethics

All animal procedures were reviewed and approved by the Institutional Animal Care and Use Committee of Washington University in St. Louis (Protocol NO. 21-0187), in accordance with the National Institutes of Health Guidelines for animal research.

Animal and study design

Cr.NIH (Swiss) female mice (6–8 weeks, ~25 g body weight) were purchased from Charles River Laboratory (Wilmington, MA, USA). The animals were housed in a room maintained at 22 °C and 55% relative humidity, with a 12-h/12-h light/dark cycle, and provided access to standard laboratory chow and tap water. 25 mice were randomly divided into five groups (n=5 for each group): (1) FUSIN delivery to the cortex (IN administration followed by FUS treatment targeted at the cortex); (2) FUS-BBBD delivery to the cortex (IV injection followed by FUS treatment targeted at the cortex); (3) DI to cortex; (4) IN only, and (5) FUSIN delivery to the brainstem (IN administration followed by FUS treatment targeted at the brainstem).

AAVs

AAV5-hSyn-EGFP was purchased from Addgene (#50465). The titer of the viral vectors was provided by the manufacturer as 1.2×10^{13} viral genomes (vg)/mL. The purchased AAVs were aliquot to single doses of 25 μL and stored in −80 °C. Each mouse in FUSIN, FUS-BBBD, and IN delivery group was delivered with the same volume of 24 μL of the AAVs. Each mouse in the DI group was injected with 1.2 μL of AAVs following the established protocol.[26,27]

FUSIN delivery of AAVs

An ultrasound image-guided FUS device (VIFU 2000; Alpinion US Inc., Bothell, WA, USA) was used for the FUSIN treatment. The FUS transducer had a center frequency of 1.5 MHz, a focal depth of 60 mm, an aperture of 60 mm, and a circular central opening of 38 mm. The transducer was coupled with a water balloon for the acoustic coupling. An ultrasound imaging probe was inserted in the central opening and co-axially aligned with the FUS transducer. The FUS transducer was driven by a built-in signal generator. The pressure amplitudes and beam profiles of the FUS transducer were calibrated regularly in a water tank filled with degassed water at room temperature using a hydrophone (HGL-200, Onda Corporation, Sunnyvale, CA). For the calibration, the hydrophone was connected to a pre-amplifier (AG-20 × 0, Onda Corporation, Sunnyvale, CA, USA) and a digital oscilloscope (Picoscope 5443D, St. Neots, United Kingdom). The FUS transducer was mounted to a 3D stage (Velmex, Lachine, QC, Canada) for moving the transducer in the water tank. The calibration was conducted by driving the FUS transducer with a 20-cycle pulsed wave with a pulse repetition frequency of 100 Hz. The full width at half maximum (FWHM) of the FUS transducer was found to be 0.6 mm × 6.0 mm in the lateral direction and axial direction, respectively. The acoustic pressure reported in this study was the measured maximum peak negative pressure at the focus after 18% reduction to take into consideration of mouse skull insertion loss.[28]

For the FUSIN treatment, mice were placed supine on a curved holder under 1.5% isoflurane anesthetization. Drops (3 μL for each drop) of AAV5-hSyn-EGFP suspended in a buffer (PBS + 0.001% Pluronic F-68 + 200 mM NaCl) were administered to the mouse by alternating between the left or right nostrils every 2 min.[24] Those drops were placed at the opening of the nostril, allowing the animal to snort each drop into the nasal cavity. After IN administration, each mouse was positioned in a stereotaxic frame (David Kopf Instruments, Tujunga, CA, USA) in a prone position with its head stabilized on the stereotaxic frame. The fur on the mouse head was removed while the scalp and the skull

remained intact. A plastic water container filled with degassed and deionized water was placed and coupled with degassed ultrasound gel on the mouse head. The bottom of the container featured a window sealed with an acoustically and optically transparent membrane (Tegaderm, 3M, St. Paul, MN, USA). Targeting specific brain location was achieved under the guidance of B-mode ultrasound imaging with the assistance of a metal grid.[28,29] The grid was positioned in the water container on top of the mouse head with the crossing point in alignment with the lambda, an anatomic landmark on the skull and visible through the mouse skin on the head. The B-mode imaging probe was used to scan through the grid to identify the crossing point of the grid. The crossing point was then used as the reference point for targeting the FUS to the cortex and brainstem on the right side of the mouse brain based on their stereotactic location relative to the lambda (Cortex: 6.0 mm frontal and 0.8 mm to the right; Brainstem: 1.0 mm posterior and 1.3 mm to the right). The depth of FUS focus was adjusted to be 0.5 mm and 4.0 mm from the skull by measuring the distance from the skull on the B-mode images for cortex and brainstem, respectively. Size-isolated microbubbles (median diameter: 4–5 μm; concentration: ~8×10^8 # of microbubbles/mL; injection volume: 30 μL) manufactured in-house[30] were injected through the tail vein, immediately followed by FUS sonication. FUS sonication was performed at 0.5 h after IN administration using the following parameters: pressure = 0.43 MPa, pulse length = 6.7 ms, pulse repetition frequency = 5 Hz, duration = 1 min and I_{spta}= 0.21 W/cm². Four points located at the corners of a square with a side length of 0.6 mm were treated.[31] Four weeks following FUSIN delivery, each mouse was sacrificed and transcardially perfused with PBS. The mouse brains and other major organs were harvested for further analysis.

FUS-BBBD delivery of AAVs

The experimental procedure for FUS-BBBD delivery of AAVs was the same as in FUSIN delivery, with the only difference being that the AAV5-hSyn-EGFP was administered by IV injection following a similar protocol used by others for FUS-BBBD delivery of AAVs.[32,33] In brief, the AAV5-hSyn-EGFP was injected into the mouse, followed by microbubble injection and then FUS sonication targeting at the cortex. The microbubble dose and FUS parameter were kept the same as those used in FUSIN delivery. Mice were sacrificed four weeks after FUS-BBBD delivery. Brain and major organs were collected for further analysis.

DI of AAVs

Mice were anesthetized via intramuscular injection of ketamine (0.10 mg/g body weight) and xylazine (0.01 mg/g body weight) mixture. Before the virus injection, buprenorphine (buprenex, 0.1 μg/g body weight) and carprofen (Rimadyl, 5 μg/g body weight) were injected subcutaneously. Coordinates used for DI into the cortex were determined according to the mouse brain atlas. 1.2 μL of AAV5-hSyn-EGFP was injected into the cortex of the mice using a microinjector (Nanoject II; Drummond Scientific) at a speed of 0.69 μL/min. After the injection, the syringe was slowly withdrawn at a speed of 0.5 mm/min. The scalp was closed with vetbond (3M) and sutured, and the mouse was allowed to recover on a heating pad. Following the surgery, sulfamethoxazole (1 mg/ml), trimethoprim (0.2 mg/ml) and carprofen (0.1 mg/ml) were chronically administered in the drinking water throughout the experiment for anti-inflammatory and antibiotic purpose. Mice were sacrificed at four weeks following DI. Brain and major organs were collected for further analysis.

Immunohistological staining of neurons

Mouse brains were harvested and fixed in 4% Paraformaldehyde (PFA) overnight and prepared for cryosectioning. The brains were first cut along the midline. The FUS-targeted side of the brain was sliced into 1 mm sections using the brain matrix (RBM-2000C; ASI Instruments, Inc., Warren, MI, USA). The slice that is 1-mm from the midline containing the cortex and brainstem, where FUS was targeted, was sectioned to 20 μm slices using a cryostat (VT1000s, Leica). For the neuron staining, the slices were preprocessed in 0.3% v/v Triton X-100 and 3% v/v blocking serum solution in PBS for 1 h in the dark at room temperature to increase the permeability and block the background. Then the slices were washed 3 times with PBS and incubated with anti-NeuN (Abcam, Cat: 104225, 1:1000) overnight at 4 °C. After 3x PBS washes, the slices were then incubated with a secondary antibody (Donkey antirabbit Alexa Fluor 594, Jackson laboratory, 1:400) in the dark for 3 h at room temperature. Finally, the slices were moved onto glass slides and mounted with VECTASHIELD (Vector Laboratories). The staining was performed by an experimenter blinded to experimental conditions. The slices were then imaged by nanozoomer (Hamamatsu Photonics, Hamamatsu City, Japan) with the 20x lens.

EGFP transgene concentration quantification with ddPCR

Genomic DNA (gDNA) was extracted from fixed-frozen mouse brain slices and fresh-frozen mouse organs using QIAamp DNA FFPE Tissue Kit (Qiagen, #56404) according to the manufacturer's instructions. The concentration and purity of gDNA were measured using the NanoDrop spectrophotometer (Thermo Fisher Scientific, Wilmington, DE, USA). The gDNA is diluted to 5–20 ng/μL for droplet digital polymerase chain reaction (ddPCR) analysis to quantify AAV EGFP transgene copies from different mouse tissues. The forward and reverse primer sequences for EGFP are 5′- GACCACTACCAGCAGAACACC -3′ and 5′- CCAGCAGGACCATGTGATCG -3′, respectively. ddPCR reactions were

conducted using Bio-Rad Q200X according to the manufacturer's instructions (Bio-Rad, Hercules, CA, USA). ddPCR reactions were prepared with 2x ddPCR™ EvaGreen Supermix (Bio-Rad, Hercules, CA, USA), 2 μL of target gDNA product, 0.1 μM forward, and reverse primers. The QX200 manual droplet generator (Bio-Rad, Hercules, CA, USA) was used to generate droplets. The PCR step was performed on a C1000 Touch Thermal Cycler (Bio-Rad, Hercules, CA, USA) by using the following program: 1 cycle at 95 °C for 10 min, 39 cycles at 95 °C for 30 s and 60°C for 1 min, 1 cycle at 4°C for 5 mins, and 1 cycle at 90 °C for 5 min, 1 cycle at 4 °C infinite hold, all at a ramp rate of 2 °C/s. Data were acquired on the QX200 droplet reader (Bio-Rad, Hercules, CA, USA) and analyzed using QuantaSoft Analysis Pro (Bio-Rad, Hercules, CA, USA). All results were manually reviewed for false positive and background noise droplets based on negative and positive control samples. EGFP transgene copies (EGFP copies/ng gDNA) were calculated by dividing the concentration (provided by QuantaSoft) by the amount of input gDNA. The ddPCR evaluation was performed by an experimenter without knowledge of the experimental conditions.

In situ hybridization (ISH)

The RNAscope assay, a novel RNA ISH technology with a unique probe design strategy that allows simultaneous signal amplification and background suppression, was used to detect the EGFP RNA molecules. ISH was performed using RNAscope Multiplex Fluorescent Reagent Kit v2 (Cat. No. 320293, ACDBio, California, USA) according to the manufacturer's directions for fixed frozen tissue. Briefly, 20-μm brain tissue sections were baked for 30 min at 60 °C prior to incubation in cold 4% PFA for 15 min. Slides were then dehydrated in 50%, 70%, and 100% ethanol for 5 min each at room temperature (RT). Then H_2O_2 was added for 10 min at RT. Target retrieval was performed using mild boil water for 10 min at 98–102 °C, followed by Protease III treatment for 30 min at 40 °C in a HybEZ Oven (ACDBio). Probes EGFP C1 (catalog #400281, ACDBio) was hybridized for 2 h at 40 °C in the HybEZ Oven, followed by amplification and detection according to the manufacturer's instructions. OPAL 620 fluorophore (catalog #FP1495001KT, Akoya Biosciences) was reconstituted according to the manufacturer's instructions and diluted in the provided TSA buffer in 1:1000 concentrations. The slices were mounted with VECTASHIELD antifade mounting media (Vector Laboratories, Burlingame, CA, USA) containing DAPI and stored at 4°C until image analysis. The fluorescent signal emanating from the EGFP RNA probe was imaged using an inverted fluorescence microscope (BZ-9000; Keyence, Osaka, Japan) with 2x and 40x objectives. The EGFP images were taken before the ISH staining process and overlaid with the ISH images using the BZ-II analyzer software version 2.2.

Fluorescence quantification

Quantification of spatial fluorescence distribution of EGFP signal and stained EGFP RNA signal was performed using a customized MATLAB program.[34] First, the brain atlas[35] was registered to the fluorescence microscopic images with DAPI staining. The registration was performed using the Control Point Registration function in MATLAB (Mathworks Inc., Natick, MA, USA). Specifically, 8 control points were selected on both the whole-brain DAPI image and the corresponding brain atlas image. The atlas was translated and rotated to align these two images using the selected control points. The transformed atlas image was then applied to the corresponding EGFP and RNAscope images. After registration, different brain regions were identified according to the brain atlas. The mean signal intensities of EGFP protein and RNA were calculated for all the identified brain regions.

Statistical analysis

Statistical analysis was performed using GraphPad Prism (Version 8.3, La Jolla, CA, USA). Differences between multiple groups were determined by one-way ANOVA followed by Bonferroni's multiple comparison test. All groups passed the normality test. *P-value* < 0.05 was considered statistically significant.

Role of funding source

The funders played no part in the design, data collection, data analyses, interpretation, writing of report or in the decision to publish the results.

Results

FUSIN noninvasively enhanced AAV delivery to the cortex

We first demonstrated that FUSIN achieved efficient delivery of AAV5-hSyn-EGFP to a superficial brain target – cortex. AAVs were administered via intranasal delivery at a total volume of 24 μL and titer of 1.2×10^{13} vg/mL to the nose. Microbubbles were administered via tail vein injection, followed by FUS sonication targeting at the cortex. The animals were sacrificed one month later, and their brains were harvested and prepared for ex vivo fluorescence imaging. A representative fluorescence image of the ex vivo mouse brain slice in the sagittal view is presented in Figure 2a. The EGFP fluorescence signal observed in the targeted cortical area indicated that AAV5-hSyn-EGFP was successfully delivered by FUSIN and subsequently expressed the carried gene. Neuron-specific EGFP expression was

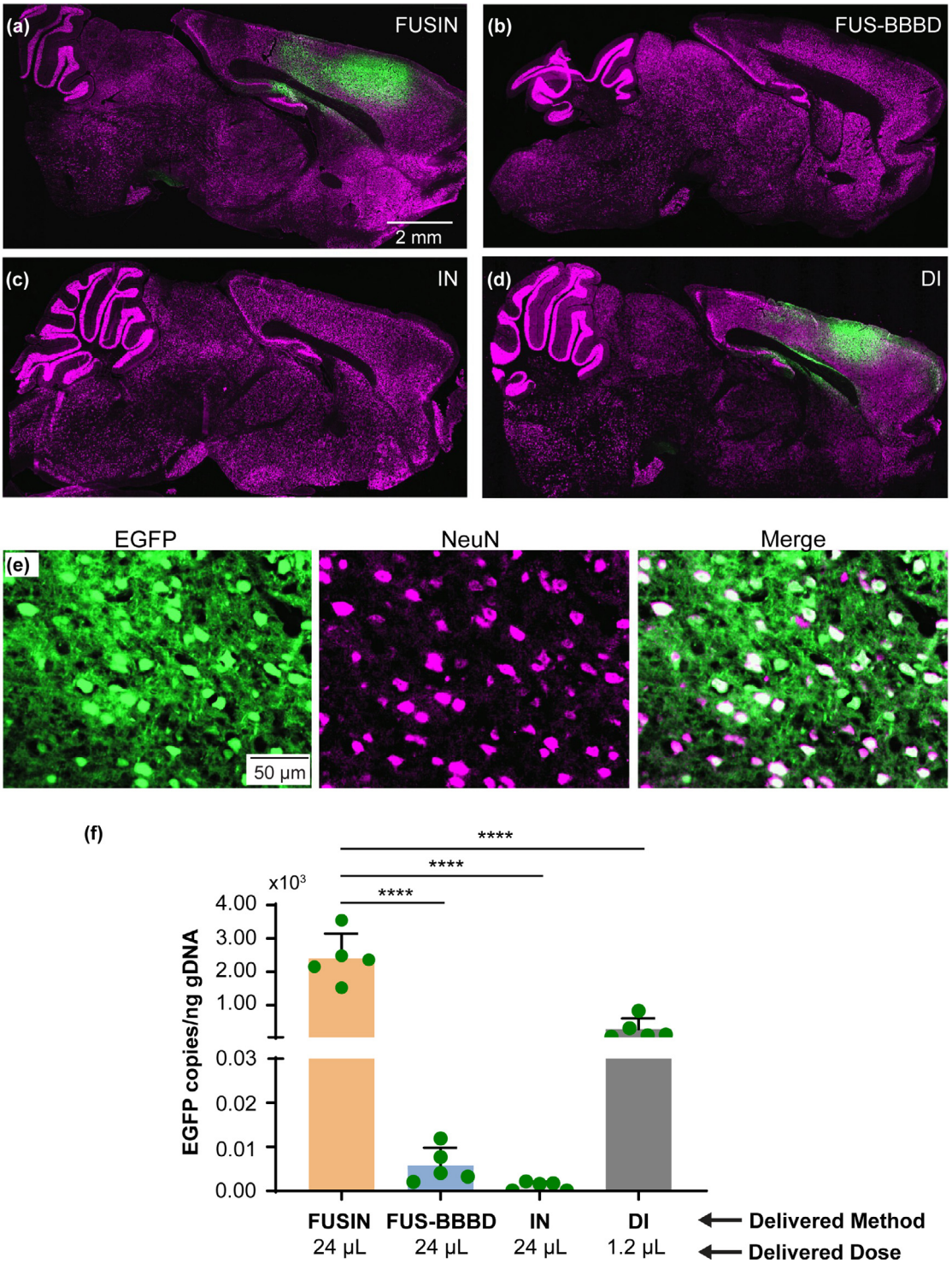

Figure 2. FUSIN significantly enhanced AAV5-hSyn-EGFP delivery to the mouse cortex.

(a–d) Representative fluorescence images of mouse brain slices in the sagittal view after FUSIN, FUS-BBBD, IN, and DI delivery of AAV5-hSyn-EGFP, respectively. FUS was targeted at the cortex for FUSIN and FUS-BBBD. DI also was targeted at the cortex. All images have the same exposure time and dynamic range. Green, EGFP; Magenta, NeuN. (e) EGFP expression was spatially colocalized with NeuN-stained neurons. Green, EGFP; Magenta, NeuN. (f) Comparisons of EGFP transgene concentrations (copies per ng of gDNA) in the mouse brain for all treatment groups ($N = 5$) (****$P < 0.0001$, one-way ANOVA followed by Bonferroni's multiple comparison test).

verified by the colocalization of EGFP with NeuN stained cells (Figure 2e).

We performed a comparative analysis of FUSIN, DI, FUS-BBBD, and IN delivery of AAV5-hSyn-EGFP. The AAV dose used in DI was limited by the injection volume (1.2 μL),[26,27] and the injection was targeted at the mouse cortex. The AAV dose for all other methods was 24 μL. FUS sonication parameters were identical for FUSIN and FUS-BBBD. Representative fluorescence images of the ex vivo mouse brain slices from FUS-BBBD, IN, and DI are presented in Figure 2b–d, respectively. EGFP expression levels were comparable for FUSIN (Figure 2a) and DI (Figure 2d). EGFP expression was not detectable by fluorescence imaging for FUS-BBBD (Figure 2b) and IN (Figure 2c).

gDNA was extracted from the brain slices to verify the fluorescence imaging results. EGFP transgene concentration (copies per ng of gDNA) was quantified using the ddPCR method. The ddPCR quantification results revealed a significant between-group difference in EGFP transgene concentration ($n = 20$; four groups; ordinary one-way ANOVA, df = 3, $p < 0.0001$). The delivery efficiency of FUSIN was 414.9-fold higher than that of FUS-BBBD ($p < 0.0001$, one-way ANOVA followed by Bonferroni's multiple comparison test) and 2073.7-fold higher than that of IN ($p < 0.0001$, one-way ANOVA followed by Bonferroni's multiple comparison test). The EGFP transgene concentration was 8.7-fold higher for FUSIN than for DI, but the direct injection dose of AAVs was 20.0-fold lower than that of FUSIN. The ddPCR analysis detected that the EGFP transgene concentration was 5.0-fold higher for FUS-BBBD than for IN (Figure 2f).

FUSIN minimized systemic biodistribution of AAVs in major organs

Systemic toxicity is a major safety concern for AAV-mediated gene therapy. We sacrificed all mice one month after performing FUSIN, FUS-BBBD, and DI, and collected major organs (heart, lung, spleen, kidney, liver, stomach, and intestine) for ddPCR (Figure 3). We found that FUSIN was associated with much lower EGFP transgene copies in most of organs than FUS-BBBD: heart (ratio of the mean EGFP DNA concentrations, FUSIN/FUS-BBBD = 0.154, $P < 0.005$, one-way ANOVA followed by Bonferroni's multiple comparison test); spleen (FUSIN/FUS-BBBD = 0.025, $P < 0.01$, one-way ANOVA followed by Bonferroni's multiple comparison test), kidney (FUSIN/FUS-BBBD = 0.073, $P < 0.05$, one-way ANOVA followed by Bonferroni's multiple comparison test); stomach (FUSIN/FUS-BBBD = 0.200, $P < 0.05$, one-way ANOVA followed by Bonferroni's multiple comparison test); intestine (FUSIN/FUS-BBBD = 0.634, $P = 0.8001$, one-way ANOVA followed by Bonferroni's multiple comparison test); and liver (FUSIN/FUS-BBBD = 0.004, $P < 0.0001$, one-way ANOVA followed by Bonferroni's multiple comparison test). EGFP transgene accumulation in the lung was higher after FUSIN delivery than after FUS-BBBD delivery, although this difference was not statistically significant (FUSIN/FUS-BBBD = 7.821, $P = 0.2361$, one-way ANOVA followed by Bonferroni's multiple comparison test). EGFP transgene accumulation in most organs did not significantly differ after FUSIN and DI delivery: heart (FUSIN/DI = 1.436, $P = 0.9607$, one-way ANOVA followed by Bonferroni's multiple comparison test); spleen (FUSIN/DI = 3.101, $P = 0.9969$, one-way ANOVA followed by Bonferroni's multiple comparison test); kidney (FUSIN/DI = 2.078, $P = 0.9896$, one-way ANOVA followed by Bonferroni's multiple comparison test); stomach (FUSIN/DI = 1.015, $P > 0.9999$, one-way ANOVA followed by Bonferroni's multiple comparison test); intestine (FUSIN/DI = 2.447; $P = 0.7931$, one-way ANOVA followed by Bonferroni's multiple comparison test); and liver (FUSIN/DI = 0.722, $P = 0.9996$, one-way ANOVA followed by Bonferroni's multiple comparison test). EGFP transgene accumulation in the lung was higher after FUSIN delivery than after DI, although this difference was but not statistically significant (FUSIN/DI = 67.014, $P = 0.1966$, one-way ANOVA followed by Bonferroni's multiple comparison test).

FUSIN noninvasively enhanced AAV delivery to the mouse brainstem

After showing that FUSIN successfully delivered AAVs to the cortex, we performed FUSIN delivery of AAVs at a deep brain target—the brainstem—to confirm that FUSIN has the potential as a platform technique for non-invasive AAV delivery to multiple brain regions. The brainstem controls basic life functions such as breathing, hearing, taste, balance, and communication between different brain regions. The critical anatomic location of the brainstem precludes surgical intervention and limits the use of invasive drug delivery techniques. Therefore, techniques that can achieve non-invasive delivery of AAVs to the brainstem would have a significant therapeutic impact.

FUSIN delivery to the brainstem was performed using the same procedure as that for the cortex with the only difference in that the FUS transducer was targeted at the brainstem. A strong EGFP fluorescence signal at the brainstem was observed in FUSIN treated mice, indicating successfully targeted AAV delivery. As EGFP can be transported in the brain by trans-synaptic transfer,[36,37] we confirmed EGFP gene delivery and transduction by directly detecting EGFP RNA at subcellular resolution using the in situ hybridization assay (Figure 4a and 4b). These results demonstrated that AAV-transduced cells were confined within the FUS-targeted brainstem region (Figure 4a and 4b). We also quantified the fluorescence intensities of EGFP protein

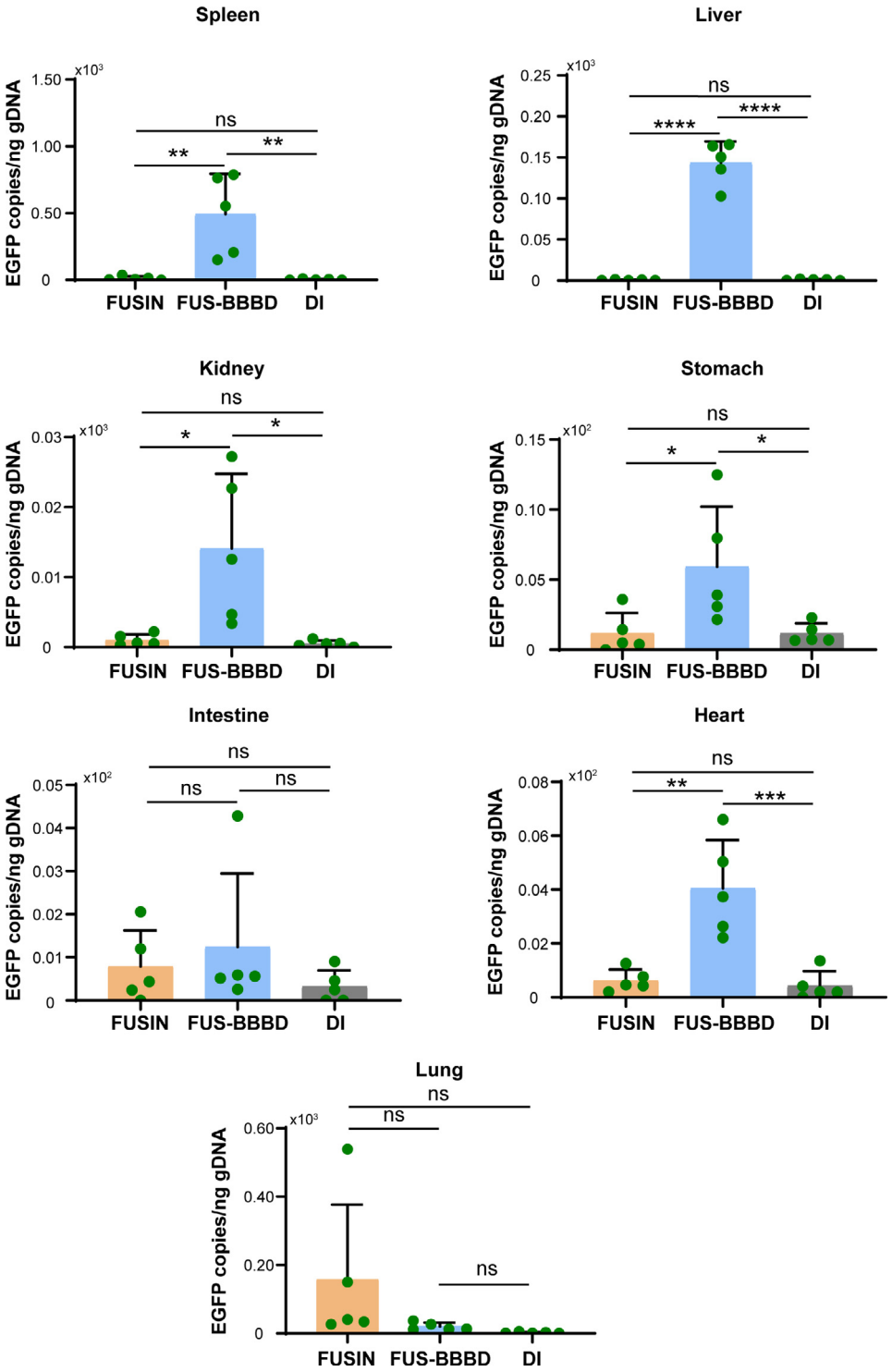

Figure 3. FUSIN minimized biodistribution of AAVs in major organs.

Comparison of EGFP transgene concentrations (copies per ng of gDNA) in major organs after FUSIN, FUS-BBBD, and DI delivery ($N = 5$ for each group) (**$P < 0.05$, **$P < 0.01$, ***$P < 0.001$, ****$P < 0.0001$, one-way ANOVA followed by Bonferroni's multiple comparison test).

and RNA. These quantification results showed higher fluorescence intensities within the brainstem region (including pons, midbrain, and medulla) than other brain areas (Figure 5). The EGFP protein and RNA signals also were observed in the cerebellum (Figures 4 and 5) because the FUS transducer used in this study had a focal region size of 0.62 × 0.62 × 6.0 mm^3 with the beam dimension in the dorsal/ventral direction to be 6 mm, which covered both the brainstem and cerebellum of the mouse brain.[29]

Discussion

Despite significant advances in gene therapies and clinical trials based on AAV vectors, no gene therapies have been approved for CNS diseases. One major challenge is the lack of non-invasive and efficient AAV delivery techniques. Here, we demonstrated that FUSIN achieved non-invasive and spatially targeted delivery of AAVs to specific FUS-targeted brain regions with high efficiency and low systemic biodistribution.

FUSIN uniquely integrates the capability of IN for non-invasive administration of AAVs and the strength of FUS combined with microbubbles for noninvasively generating mechanical forces in the brain that enhance the delivery efficiency of IN-administered agents at the FUS-targeted brain site. Preclinical studies and clinical trials have investigated IN delivery of various therapeutic agents directly from the nose to the brain bypassing the BBB; however, nasal administration is a largely unexplored approach for AAV delivery to the CNS due to its low delivery efficiency beyond the olfactory bulb.[18,19,38–41] IN delivery of AAVs was reported to have therapeutic benefits in the treatment of neurologic and psychiatric diseases in pre-clinical animal models. However, in those reports, either repeated AAV administrations were required.[40,42–44] or AAVs were intended to be deposited in the olfactory region to express enzymes that diffused to the whole brain.[19] Our previous studies showed that FUSIN achieved significantly higher efficiency than IN for delivering various therapeutic agents, including dextrans (~40 kDa molecular weight), gold nanoparticles (~4–5 nm diameter), immune checkpoint inhibitor (150 kDa), and a brain-derived neurotrophic factor (28 kDa), to different brain locations, including striatum and brainstem.[23,24,31,45] The current study expanded the application of FUSIN to the delivery of AAV vectors (~25 nm),[46] and showed that FUSIN achieved over 2000-fold higher efficiency for AAV5-hSyn-EGFP delivery to the cortex than IN delivery. This study also demonstrated that FUSIN delivery achieved a similar transduction level as DI. Although the bioavailability of DI is high, it is limited by the injection solute volume (~1 μL). IN is also limited by the solute volume (3 μL) that can be administered each time due to the limited volume of the mouse nostril. However, IN administration is non-invasive and repeated administration has partially overcome the solute volume limitation. The total volume administered in this FUSIN study was 24 μL, which is the commonly used IN administration volume for the mouse.[47] Previous studies showed that FUSIN enhanced the delivery of brain-derived neurotrophic factor (BDNF) and produced neurorestorative effects in a Parkinson's disease mouse model.[24,45] We speculate that FUSIN-mediated AAV delivery can achieve higher therapeutic efficacy than IN, and potentially be used for the treatment of various brain diseases (e.g., Parkinson's disease). However, future studies are needed to demonstrate the therapeutic efficacy of FUSIN-mediated AAV delivery.

This study showed that FUSIN achieved higher delivery efficiency of AAV5-hSyn-EGFP than the established FUS-BBBD technique when keeping all experimental parameters the same. There were no clearly detectable EGFP signals in the fluorescence images obtained from the FUS-BBBD group when the exposure time of the images was kept the same as those from the FUSIN and DI. It is possible that the EGFP fluorescence signals in the FUS-BBBD group were below the image detection limit. Indeed, the ddPCR quantification showed that FUS-BBBD increased the EGFP DNA concentration by 5-fold compared to the IN only (Figure 2f). Previous studies of FUS-BBBD delivery of AAVs demonstrated successful gene expression by immunofluorescence staining to amplify the fluorescence signal[32,48,49] or by utilizing AAV9 vectors[14,15,48] which are known to be BBB permeable.[16,32] FUS-BBBD broadened previous options for systemic AAV delivery to the brain to include serotypes that cannot innately cross the BBB. To achieve effective gene transduction, FUS-BBBD requires either the use of ultrasound parameters that are close to the limits that damage tissues[50–52] or overdosed AAV injection.[13] The AAV5 used in our study is not innately permeable through the BBB, and has never been reported in FUS-BBBD delivery studies. Our study demonstrated that FUSIN achieved over 400-fold higher AAV delivery efficiency than FUS-BBBD. This enhanced delivery was consistent with our previous study on delivering gold nanoparticles, which reported that FUSIN achieved 25.0-fold higher delivery efficiency than FUS-BBBD.[23] The mechanisms behind this observation need further investigation. IN-administered agents can directly reach the brain without undergoing first-pass metabolism. These agents distribute in the brain along the perivascular space that is beyond the BBB, whereas intravenously injected agents have to cross the BBB. FUS activation of microbubble cavitation at a targeted brain location enhances the local transportation and accumulation of AAVs that are in the perivascular space.

We showed that FUSIN delivery of AAVs significantly reduced the systemic biodistribution of the AAVs in major organs. The AAV5-hSyn-EGFP depositions, indicated by EGFP transgene concentrations, in the

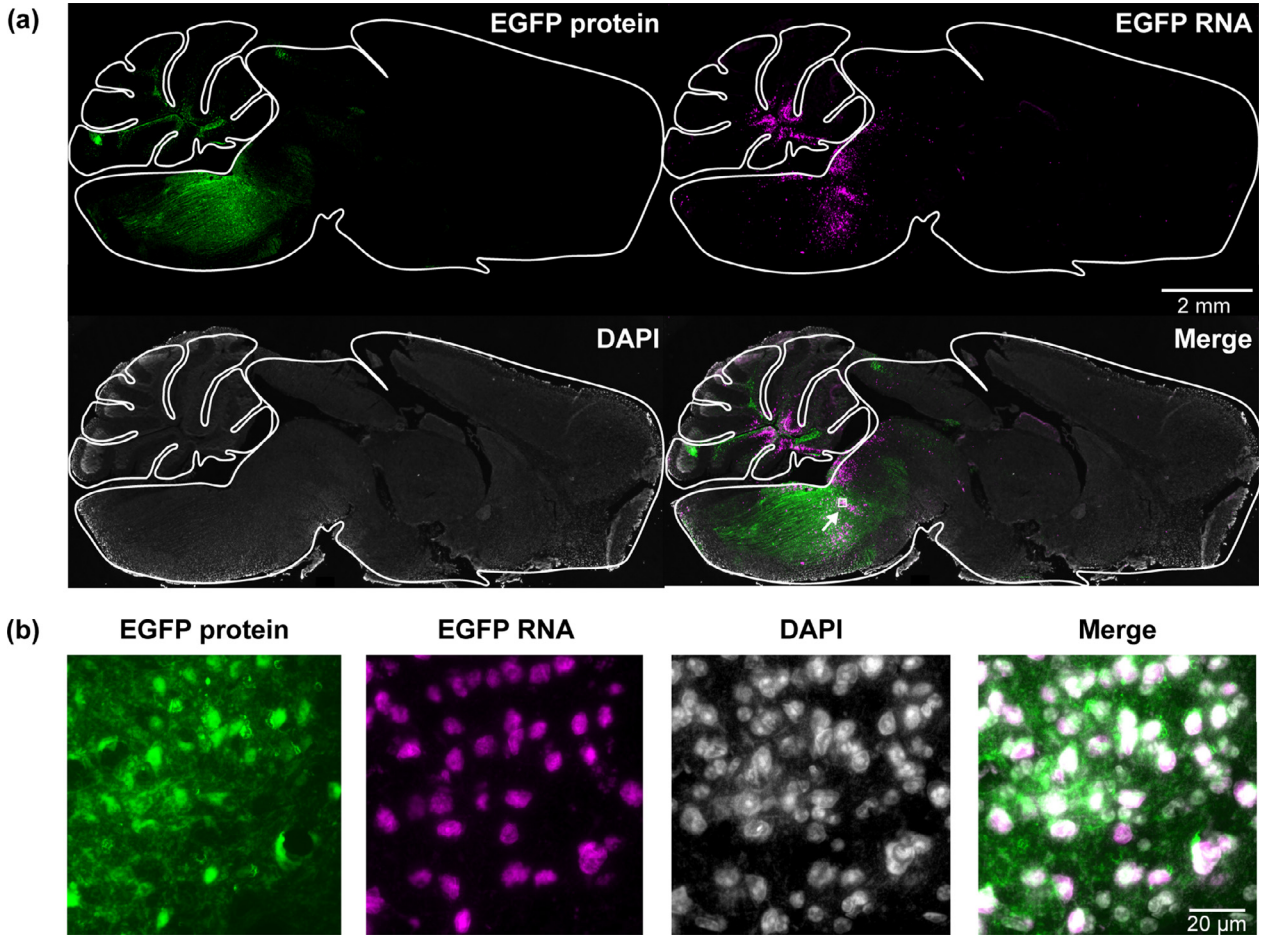

Figure 4. FUSIN delivery of AAV5-hSyn-EGFP to the mouse brainstem.

(a) Fluorescence images of representative ex vivo mouse brain slices (2 × magnification). Green color indicates EGFP expression; Magenta color indicates EGFP RNA level by in situ hybridization. (b) High-magnification image (40 × magnification) of ex vivo mouse brain slices within the white box at the brainstem region.

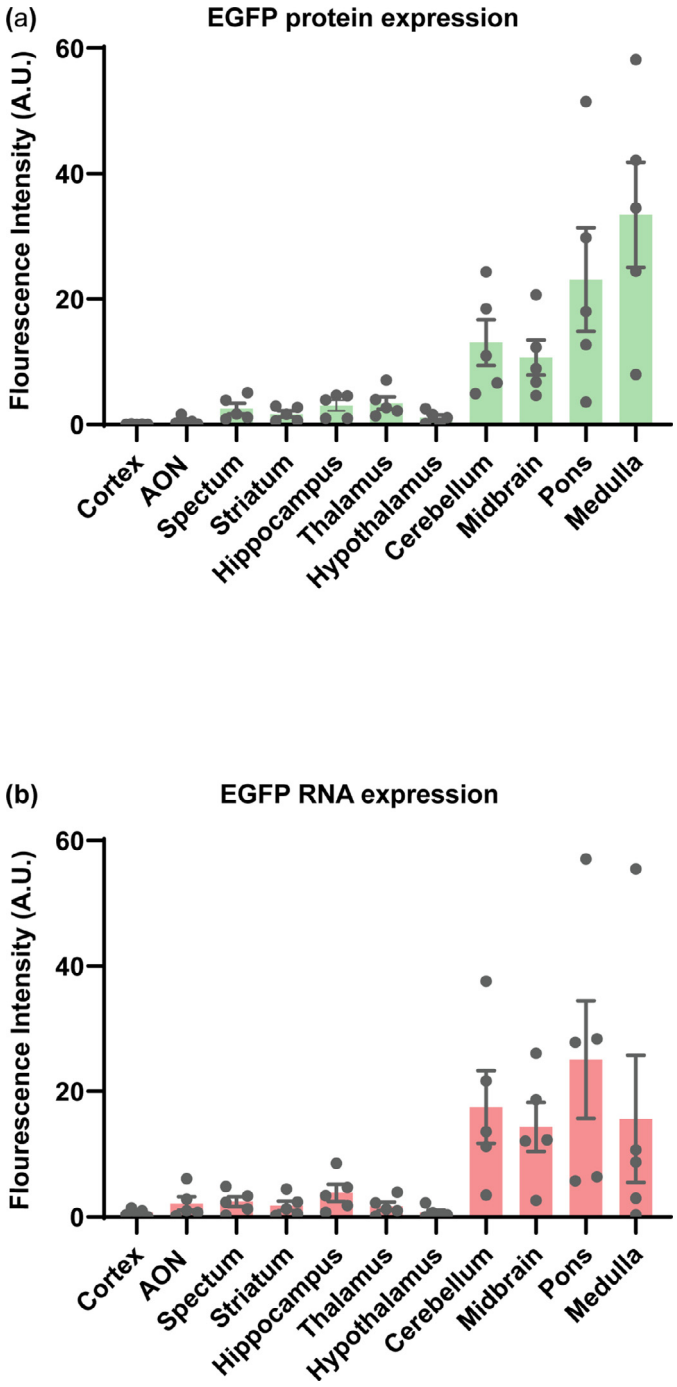

Figure 5. Quantification of EGFP protein and RNA in mouse brainstem (midbrain, pons, and medulla) and other brain regions.

Spatial quantification of fluorescence intensity of the (a) EGFP protein and (b) EGFP RNA staining. Enhanced fluorescence intensity was observed in the FUS targeted the brainstem region (including pons, midbrain, and medulla) and cerebellum region. (AON: Anterior olfactory nucleus).

heart, liver, spleen, stomach, and intestine were significantly lower after FUSIN than after FUS-BBBD, and were comparable after FUSIN and DI. Our previous studies reported low accumulation of FUSIN-delivered nanoparticles in major organs, except in the stomach and intestine, when quantified at 0.5 hours after FUSIN treatment.[23,53] The nanoparticles that accumulated in the stomach and intestine could be excreted through

feces, thereby resulting in minimal systemic toxicity. The present study did not detect high AAV concentrations in the stomach and intestine because mice were sacrificed one month after FUSIN treatment. The EGFP transgene concentration in the lung was higher with FUSIN delivery than FUS-BBBD and DI, although the differences were not statistically significant. AAV delivery and tissue/cell tropisms are highly serotype-dependent.[54] The enhanced accumulation of AAV5 in the lung by FUSIN might be due to the specific characteristic of AAV5 that is prone to affect the lung after IN administration.[55,56] The lung transfection might be reduced or avoided by using a different serotype. Additionally, we expect that FUSIN would have comparable low immunogenicity as DI and much lower immunogenicity than FUS-BBBD and IV. Future studies are needed to evaluate the immunogenicity associated with FUSIN-mediated AAV delivery and compare it with other delivery methods.

Current AAV-based gene therapy for CNS diseases has primarily relied on DI. However, the development of AAV therapies by DI has been hindered by the challenges in safely achieving widespread gene expression in the brain. Multiple injections are needed to cover a large brain region, which further increases the risk associated with DI.[57,58] We showed that FUSIN could achieve non-invasive AAV delivery to FUS-targeted brain regions, regardless of superficial or deep brain, and this technique has the potential to replace DI. Instead of drilling multiple holes in the skull for DI, FUS can easily target multiple brain sites by mechanical moving the FUS transducer or electronically steering the beam focus for non-invasive drug delivery to a large brain region.[59]

FUS has emerged as a new class of therapies for the clinical treatment of CNS diseases. FUS-induced BBB disruption for the delivery of intravenously injected therapeutic drugs has been demonstrated as safe and feasible in patients with brain diseases such as glioblastoma,[9,10] Alzheimer's disease,[11] and amyotrophic lateral sclerosis (ALS).[12] IN delivery has been used in multiple clinical studies to deliver small molecule agents to the brain, including oxytocin,[60] insulin,[61] erythropoietin,[62] perillyl alcohol,[63] and neurotrophic factor,[64,65] for the treatment of diseases such as neurodegeneration diseases and brain tumors. These recent technological advances have paved the way for future clinical usage of FUSIN to deliver AAVs for treating a broad range of CNS diseases by integrating FUS devices used in FUS-BBBD clinical studies with established IN administration methods.

Although this study demonstrated the great potential of FUSIN in AAV delivery to the brain, it has several limitations. First, this study only tested FUSIN delivery of AAV5. Although AAV9 has been commonly used for brain drug delivery because it can permeate through the BBB,[46] we selected AAV5 to demonstrate that FUSIN is capable of delivering non-BBB permeable AAV vectors. Future work will investigate the impact of AAV serotype on FUSIN delivery outcome. Second, this study used FUS parameters previously optimized for delivering a model agent (albumin) to brainstem.[31] However, the delivery outcome could differ for different brain regions when the same treatment parameters are used. The distance of the targeted brain region to the IN administration entry points in the brain (i.e., olfactory bulb and brainstem) could affect the kinetics and amount of IN-administered agents that can reach the target.[21] The efficiency of FUSIN delivery of AAVs could be improved by specifically optimizing the FUSIN treatment parameters for each targeted brain region. Third, the FUS transducer used in this study was a commercially available device similar to those typically used in FUS-mediated drug delivery. Customized FUS transducers with a small focal region size[66] can be used in the future to improve the spatial precision in AAV delivery. Fourth, although this study demonstrated enhanced AAV delivery to the brain and minimal systemic exposure, suggesting that FUSIN has great potential as a platform technique for gene therapy of brain disease, future studies are needed to evaluate the therapeutic benefits FUSIN in the treatment of specific brain diseases.

In summary, the lack of non-invasive methods for efficient delivery of AAVs to the brain with minimal systemic toxicity limits the development of CNS gene therapy. This study demonstrated a new method that combines FUS with intranasal administration (FUSIN) of AAVs could achieve efficient AAV delivery and gene transduction at the FUS-targeted brain region with minimal biodistribution of the AAVs to other major organs. Findings from this study suggest that FUSIN is a promising technology for AAV delivery to the brain with the potential to be translated to the clinic for the treatment of CNS diseases.

Contributors

DZY: Conceptualization, Methodology, Data Curation, Formal analysis, Investigation, Writing - Original Draft, Visualization; JYY: Methodology, Data Curation, Validation, Writing - Review & Editing; YHY: Software, Formal analysis, Validation, Writing - Review & Editing; YMY: Methodology, Data Curation; ZTH: Software, Formal analysis, Writing - Review & Editing;Siaka Fadera: Methodology; HC: Conceptualization, Resources, Writing - Review & Editing, Visualization, Supervision, Project administration, Funding acquisition. DZY, JYY, YHY and HC have verified the underlying data. All the authors read and approved the final manuscript.

Data sharing statement

The data supporting the conclusions of this study are available within the article. Raw data files will be made available by inquiries to the corresponding author (hongchen@wustl.edu).

Declaration of interests

The authors declare no conflict of interest.

Acknowledgments

This research was funded by the National Institutes of Health (NIH) grants R01EB027223, R01EB030102, R01MH116981, and UG3MH126861.

References

1 Bain L, Stroud C. *Advancing Gene-Targeted Therapies for Central Nervous System Disorders*. editors. Washington, D.C.: National Academies Press; 2019. https://doi.org/10.17226/25529.
2 Piguet F, Alves S, Cartier N. Clinical gene therapy for neurodegenerative diseases: past, present, and future. *Hum Gene Ther*. 2017;28:988–1003.
3 Albert K, Voutilainen MH, Domanskyi A, Airavaara M. AAV vector-mediated gene delivery to substantia nigra dopamine neurons: implications for gene therapy and disease models. *Genes (Basel)*. 2017;8:1–15.
4 Taghian T, Marosfoi MG, Puri AS, et al. A safe and reliable technique for CNS delivery of AAV vectors in the cisterna magna. *Mol Ther*. 2020;28:411–421.
5 Matsuzaki Y, Konno A, Mochizuki R, et al. Intravenous administration of the adeno-associated virus-PHP.B capsid fails to upregulate transduction efficiency in the marmoset brain. *Neurosci Lett*. 2018;665:182–188.
6 Liguore WA, Domire JS, Button D, et al. AAV-PHP.B administration results in a differential pattern of CNS biodistribution in non-human primates compared with mice. *Mol Ther*. 2019;27:2018–2037.
7 Peng KW, Pham L, Ye H, et al. Organ distribution of gene expression after intravenous infusion of targeted and untargeted lentiviral vectors. *Gene Ther*. 2001;8:1456–1463.
8 Ganesan LP, Mohanty S, Kim J, Clark KR, Robinson JM, Anderson CL. Rapid and efficient clearance of blood-borne virus by liver sinusoidal endothelium. *PLoS Pathog*. 2011;7:e1002281.
9 Carpentier A, Canney M, Vignot A, et al. Clinical trial of blood-brain barrier disruption by pulsed ultrasound. *Sci Transl Med*. 2016;8:343re2.
10 Park SH, Kim MJ, Jung HH, et al. Safety and feasibility of multiple blood-brain barrier disruptions for the treatment of glioblastoma in patients undergoing standard adjuvant chemotherapy. *J Neurosurg*. 2021;134:475–483.
11 Lipsman N, Meng Y, Bethune AJ, et al. Blood–brain barrier opening in Alzheimer's disease using MR-guided focused ultrasound. *Nat Commun*. 2018;9:2336.
12 Abrahao A, Meng Y, Llinas M, et al. First-in-human trial of blood-brain barrier opening in amyotrophic lateral sclerosis using MR-guided focused ultrasound. *Nat Commun*. 2019;10:4373.
13 Wang S, Olumolade OO, Sun T, Samiotaki G, Konofagou EE. Noninvasive, neuron-specific gene therapy can be facilitated by focused ultrasound and recombinant adeno-associated virus. *Gene Ther*. 2015;22:104–110.
14 Thévenot E, Jordão JF, O'Reilly MA, et al. Targeted delivery of self-complementary adeno-associated virus serotype 9 to the brain, using magnetic resonance imaging-guided focused ultrasound. *Hum Gene Ther*. 2012;23:1144–1155.
15 Szablowski JO, Lee-Gosselin A, Lue B, Malounda D, Shapiro MG. Acoustically targeted chemogenetics for the non-invasive control of neural circuits. *Nat Biomed Eng 2018 27*. 2018;2:475–484.
16 Kofoed RH, Heinen S, Silburt J, et al. Transgene distribution and immune response after ultrasound delivery of rAAV9 and PHP.B to the brain in a mouse model of amyloidosis. *Mol Ther - Methods Clin Dev*. 2021;23:390–405.
17 Lochhead JJ, Thorne RG. Intranasal delivery of biologics to the central nervous system. *Adv Drug Deliv Rev*. 2012;64:614–628.
18 Wolf DA, Hanson LR, Aronovich EL, et al. Lysosomal enzyme can bypass the blood-brain barrier and reach the CNS following intranasal administration. *Mol Genet Metab*. 2012;106:131–134.
19 Belur LR, Temme A, Podetz-Pedersen KM, et al. Intranasal adeno-associated virus mediated gene delivery and expression of human iduronidase in the central nervous system: a noninvasive and effective approach for prevention of neurologic disease in mucopolysaccharidosis Type i. *Hum Gene Ther*. 2017;28:576–587.
20 Chen H, Li X, Wan M, Wang S. High-speed observation of cavitation bubble clouds near a tissue boundary in high-intensity focused ultrasound fields. *Ultrasonics*. 2009;49:289–292.
21 Kumar NN, Lochhead JJ, Pizzo ME, et al. Delivery of immunoglobulin G antibodies to the rat nervous system following intranasal administration: distribution, dose-response, and mechanisms of delivery. *J Control Rel*. 2018;286:467–484.
22 Lochhead JJ, Davis TP. Perivascular and perineural pathways involved in brain delivery and distribution of drugs after intranasal administration. *Pharmaceutics*. 2019;11. https://doi.org/10.3390/pharmaceutics11110598.
23 Ye D, Zhuang X, Yue Y, et al. Comparison of focused ultrasound-mediated intranasal delivery and focused ultrasound-induced blood-brain barrier disruption in the delivery of gold nanoclusters to the brainstem. *IEEE international ultrasonics symposium IUS*. 2018—January;2018:5–8.
24 Chen H, Yang GZX, Getachew H, Acosta C, Sierra Sánchez C, Konofagou EE. Focused ultrasound-enhanced intranasal brain delivery of brain-derived neurotrophic factor. *Sci Rep*. 2016;6:28599.
25 Sultan D, Ye D, Heo GS, et al. Focused ultrasound enabled trans-blood brain barrier delivery of gold nanoclusters: effect of surface charges and quantification using positron emission tomography. *Small*. 2018;14:1703115.
26 Yang Y, Pacia CP, Ye D, et al. Sonothermogenetics for noninvasive and cell-type specific deep brain neuromodulation. *Brain Stimul*. 2021;14:790–800.
27 Kravitz AV, Freeze BS, Parker PRL, et al. Regulation of parkinsonian motor behaviours by optogenetic control of basal ganglia circuitry. *Nature*. 2010;466:622–626.
28 Choi JJ, Pernot M, Small S a, Konofagou EE. Noninvasive, transcranial and localized opening of the blood-brain barrier using focused ultrasound in mice. *Ultrasound Med Biol*. 2007;33:95–104.
29 Ye D, Sultan D, Zhang X, et al. Focused ultrasound-enabled delivery of radiolabeled nanoclusters to the pons. *J Control Rel*. 2018;283:143–150.
30 Feshitan J a, Chen CC, Kwan JJ, Borden M a. Microbubble size isolation by differential centrifugation. *J Colloid Interface Sci*. 2009;329:316–324.
31 Ye D, Luan J, Pang H, et al. Characterization of focused ultrasound-mediated brainstem delivery of intranasally administered agents. *J Control Rel*. 2020;328:276–285.
32 Weber-Adrian D, Kofoed RH, Silburt J, et al. Systemic AAV6-synapsin-GFP administration results in lower liver biodistribution, compared to AAV1&2 and AAV9, with neuronal expression following ultrasound-mediated brain delivery. *Sci Rep*. 2021;11:1–13.
33 Noroozian Z, Xhima K, Huang Y, et al. MRI-guided focused ultrasound for targeted delivery of rAAV to the brain. *Methods Mol Biol*. 2019;1950:177–197.
34 Yang Y, Zhang X, Ye D, et al. Cavitation dose painting for focused ultrasound-induced blood-brain barrier disruption. *Sci Rep*. 2019;9:2840.
35 Paxinos G, KBF. *The Mouse Brain in Stereotaxic Coordinates*. Gulf Professional Publishing; 2004.
36 Maskos U, Kissa K, St. Cloment C, Brûlet P. Retrograde trans-synaptic transfer of green fluorescent protein allows the genetic mapping of neuronal circuits in transgenic mice. *Proc Natl Acad Sci USA*. 2002;99:10120–10125.
37 Salegio EA, Cukrov M, Lortz R, et al. Feasibility of targeted delivery of AAV5-GFP into the cerebellum of nonhuman primates following a single convection-enhanced delivery infusion. *Hum Gene Ther*. 2022;33:86–93.
38 Quinn K, Quirion MR, Lo CY, Misplon JA, Epstein SL, Chiorini JA. Intranasal administration of adeno-associated virus type 12 (AAV12) leads to transduction of the nasal epithelia and can initiate transgene-specific immune response. *Mol Ther*. 2011;19:1990–1998.
39 Williams CL, Uytingco CR, Green WW, et al. Gene therapeutic reversal of peripheral olfactory impairment in bardet-biedl syndrome. *Mol Ther*. 2017;25:904–916.
40 Ma XC, Liu P, Zhang XL, et al. Intranasal delivery of recombinant AAV containing BDNF fused with HA2TAT: a potential promising therapy strategy for major depressive disorder. *Sci Rep*. 2016;6. https://doi.org/10.1038/srep22404.
41 Belur LR, Romero M, Lee J, et al. Comparative effectiveness of intracerebroventricular, intrathecal, and intranasal routes of AAV9 vector administration for genetic therapy of neurologic disease in

murine mucopolysaccharidosis type I. *Front Mol Neurosci*. 2021;14. https://doi.org/10.3389/FNMOL.2021.618360.
42 Liu F, Liu Y, Lei G, et al. Antidepressant effect of recombinant NT4-NAP/AAV on social isolated mice through intranasal route. *Oncotarget*. 2017;8:10103–10113.
43 Qi B, Yang Y, Cheng Y, et al. Nasal delivery of a CRMP2-derived CBD3 adenovirus improves cognitive function and pathology in APP/PS1 transgenic mice. *Mol Brain*. 2020;13. https://doi.org/10.1186/S13041-020-00596-3.
44 Chen C, Dong Y, Liu F, et al. A study of antidepressant effect and mechanism on intranasal delivery of BDNF-HA2TAT/AAV to rats with post-stroke depression. *Neuropsychiatr Dis Treat*. 2020;16:637–649.
45 Ji R, Smith M, Niimi Y, et al. Focused ultrasound enhanced intranasal delivery of brain derived neurotrophic factor produces neurorestorative effects in a Parkinson's disease mouse model. *Sci Rep*. 2019;9:19402.
46 Merkel SF, Andrews AM, Lutton EM, et al. Trafficking of adeno-associated virus vectors across a model of the blood-brain barrier; a comparative study of transcytosis and transduction using primary human brain endothelial cells. *J Neurochem*. 2017;140:216–230.
47 Hanson LR, Fine JM, Svitak AL, Faltesek KA. Intranasal Administration of CNS therapeutics to awake mice. *J Vis Exp*. 2013:1–7.
48 Wang S, Kugelman T, Buch A, et al. Non-invasive, focused ultrasound-facilitated gene delivery for optogenetics. *Sci Rep*. 2017;7:39955.
49 Xhima K, Nabbouh F, Hynynen K, Aubert I, Tandon A. Noninvasive delivery of an α-synuclein gene silencing vector with magnetic resonance–guided focused ultrasound. *Mov Disord*. 2018;33:1567–1579.
50 Hsu P-H, Wei K-C, Huang C-Y, et al. Noninvasive and targeted gene delivery into the brain using microbubble-facilitated focused ultrasound. *PLoS One*. 2013;8:e57682.
51 Stavarache MA, Petersen N, Jurgens EM, et al. Safe and stable noninvasive focal gene delivery to the mammalian brain following focused ultrasound. *J Neurosurg*. 2019;130:989–998.
52 Alonso A, Reinz E, Leuchs B, et al. Focal delivery of AAV2/1-transgenes into the rat brain by localized ultrasound-induced BBB opening. *Mol Ther Nucleic Acids*. 2013;2:e73.
53 Ye D, Zhang X, Yue Y, et al. Focused ultrasound combined with microbubble-mediated intranasal delivery of gold nanoclusters to the brain. *J Control Rel*. 2018;286:145–153.
54 Srivastava A. In vivo tissue-tropism of adeno-associated viral vectors. *Curr Opin Virol*. 2016;21:75.
55 Sumner-Jones SG, Davies LA, Varathalingam A, Gill DR, Hyde SC. Long-term persistence of gene expression from adeno-associated virus serotype 5 in the mouse airways. *Gene Ther*. 2006;13:1703–1713.
56 Auricchio A, O'Connor E, Weiner D, et al. Noninvasive gene transfer to the lung for systemic delivery of therapeutic proteins. *J Clin Invest*. 2002;110:499–504.
57 Janson C, McPhee S, Bilaniuk L, et al. Gene therapy of Canavan disease: AAV-2 vector for neurosurgical delivery of aspartoacylase gene (ASPA) to the human brain. *Hum Gene Ther*. 2002;13:1391–1412.
58 Tardieu M, Zérah M, Gougeon ML, et al. Intracerebral gene therapy in children with mucopolysaccharidosis type IIIB syndrome: an uncontrolled phase 1/2 clinical trial. *Lancet Neurol*. 2017;16:712–720.
59 Gong Y, Ye D, Chien CY, Yue Y, Chen H. Comparison of sonication patterns and microbubble administration strategies for focused ultrasound-mediated large-volume drug delivery. *IEEE Trans Biomed Eng*. 2022. https://doi.org/10.1109/TBME.2022.3170832.
60 Goodin BR, Anderson AJB, Freeman EL, Bulls HW, RM T, Ness TJ. Administration of intranasal oxytocin may augment endogenous pain nhibitory capacity and reduce anxiety. *Clin J Pain*. 2015;31:757–767.
61 Reger M a, Watson GS, Green PS, et al. Intranasal insulin administration dose-dependently modulates verbal memory and plasma amyloid-beta in memory-impaired older adults. *J Alzheimers Dis*. 2008;13:323–331.
62 Santos-Morales O, Díaz-Machado A, Jiménez-Rodríguez D, et al. Nasal administration of the neuroprotective candidate NeuroEPO to healthy volunteers: a randomized, parallel, open-label safety study. *BMC Neurol*. 2017;17(1). https://doi.org/10.1186/S12883-017-0908-0.
63 Da Fonseca CO, Masini M, Futuro D, Caetano R, Rocha Gattass C, Quirico-Santos T. Anaplastic oligodendroglioma responding favorably to intranasal delivery of perillyl alcohol: a case report and literature review. *Surg Neurol*. 2006;66:611–615.
64 Bellis A de, Bellis M de, Aloe L. Long-term non-invasive treatment via intranasal administration of nerve growth factor protects the human brain in frontotemporal dementia associated with corticobasal syndrome: a pilot study. *J Alzheimer's Dis Rep*. 2018;2(1):67–77.
65 Chiaretti A, Conti G, Falsini B, et al. Intranasal nerve growth factor administration improves cerebral functions in a child with severe traumatic brain injury: a case report. *Brain Inj*. 2017;31:1538–1547.
66 Hu Z, Chen S, Yang Y, Gong Y, Chen H. An affordable and easy-to-use focused ultrasound device for noninvasive and high precision drug delivery to the mouse brain. *IEEE Trans Biomed Eng*. 2022;69(9):2723–2732.